Chapter

3

THE BEHAVIOUR
OF SOLAR CELLS

3.1   EFFECT OF LIGHT

A silicon solar cell is a diode formed by joining *p*-type (typically boron doped) and *n*-type (typically phosphorous doped) silicon. Light shining on such a cell can behave in a number of ways, as illustrated in Fig. 3.1. To maximise the power rating of a solar cell, it must be designed so as to maximise desired absorption (3) and absorption after reflection (5).

The electric field $\hat{E}$ at the *p-n* junction sweeps electrons to the *n* side and holes to the *p* side. The ideal flow at short circuit is shown in Fig. 3.2. However, some electron-hole (e-h) pairs get lost before collection, as shown in Fig. 3.3.

In general, the closer the point of e-h generation to the *p-n* junction, the better the chance of 'collection'. 'Collected carriers' are those that generate a finite current when $V = 0$. Chances of collection are particularly good if the e-h pairs are generated within a *diffusion length* of the junction, as discussed in Chapter 2.

The characteristic curves generated by plotting I against V for a diode (I-V curves) were shown in Fig. 2.11 for I_0, with no light falling on the cell. Illumination of a cell merely adds to the normal 'dark' currents in the diode so that the diode law becomes

$$I = I_0 \left[\exp\left(\frac{qV}{nkT} \right) - 1 \right] - I_L \tag{3.1}$$

where I_L is the light-generated current.

The light has the effect of shifting the I-V curve down into the fourth quadrant where power can be extracted from the diode, as shown in Fig. 3.4.

The I-V curve characterises the cell, with its power output being equal to the area of the rectangle in the bottom right-hand quadrant of Fig. 3.4*a*. This I-V curve is most often shown reversed, as in Fig. 3.5, with the output curve in the first quadrant, and represented by

$$I = I_L - I_0 \left[\exp\left(\frac{qV}{nkT} \right) - 1 \right] \tag{3.2}$$
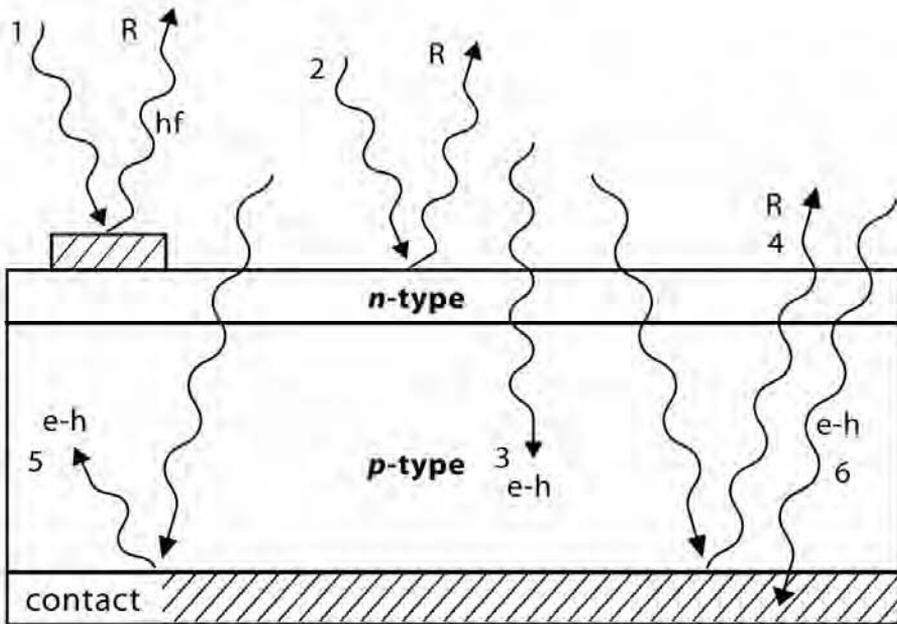
Figure 3.1. Behaviour of light shining on a solar cell. (1) Reflection and absorption at top contact. (2) Reflection at cell surface. (3) Desired absorption. (4) Reflection from rear out of cell—weakly absorbed light only. (5) Absorption after reflection. (6) Absorption in rear contact.
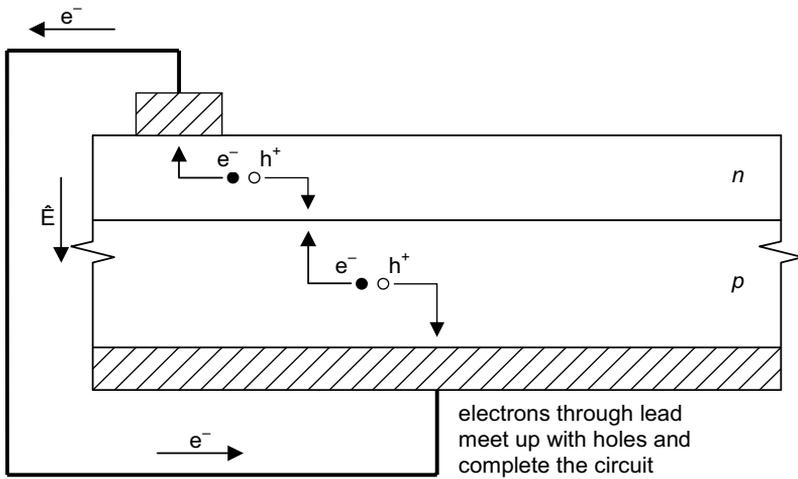
Figure 3.2. The ideal short circuit flow of electrons and holes at a *p-n* junction.
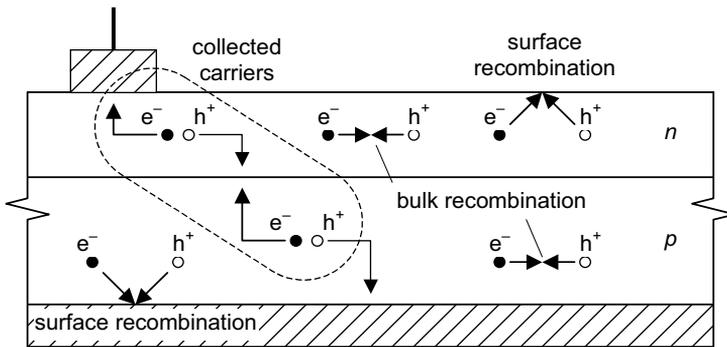
Figure 3.3. Possible modes of recombination of electron-hole pairs, showing 'collection' of carriers that do not recombine.

(*a*)   (*b*)
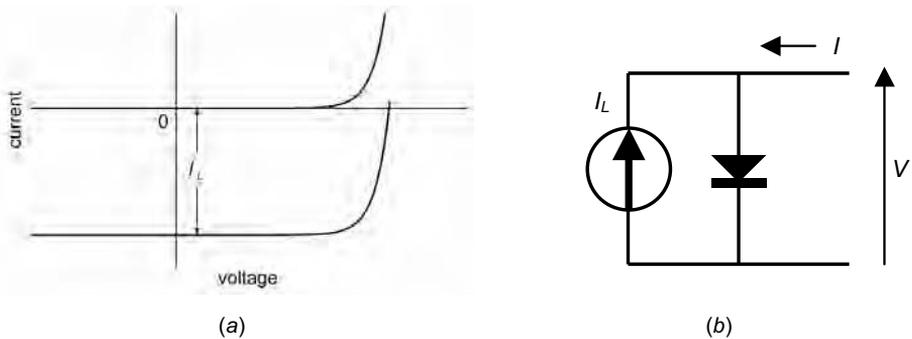
Figure 3.4. The effect of light on the current-voltage characteristics of a *p-n* junction.
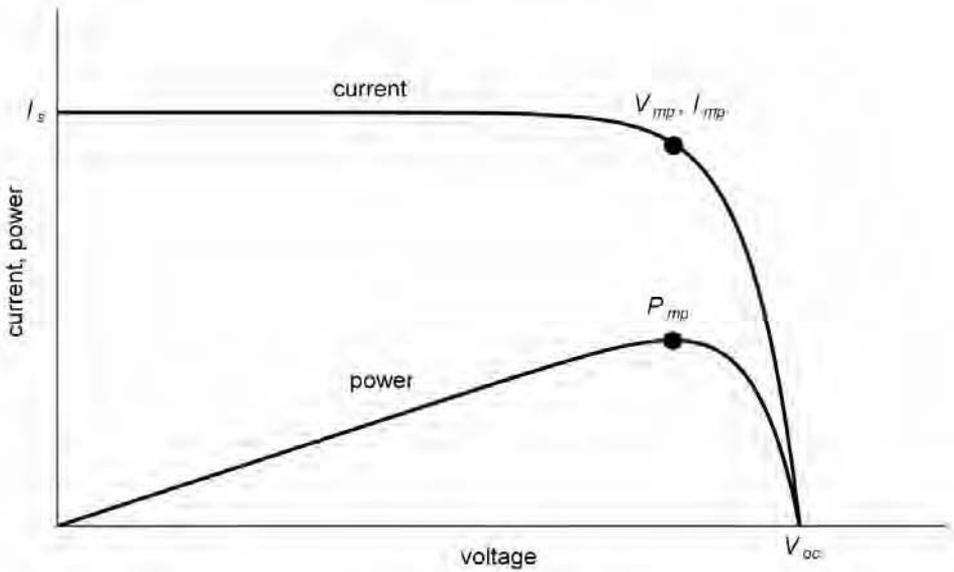
Figure 3.5. Typical representation of an I-V curve, showing short-circuit current (I_{sc} and open-circuit voltage (V_{oc}) points, as well as the maximum power point (V_{mp}, I_{mp}).

The two limiting parameters used to characterise the output of solar cells for given irradiance, operating temperature and area are (Shockley & Queisser, 1961):

1. **Short circuit current** (I_{sc})—the maximum current, at zero voltage. Ideally, if $V = 0$, $I_{sc} = I_L$. Note that I_{sc} is directly proportional to the available sunlight.

2. **Open circuit voltage** (V_{oc})—the maximum voltage, at zero current. The value of V_{oc} increases logarithmically with increased sunlight. This characteristic makes solar cells ideally suited to battery charging.

Note that at $I = 0$,

$$V_{oc} = \frac{nkT}{q}\ln\left(\frac{I_L}{I_0}+1\right) \qquad (3.3)$$

For each point on the I-V curve, the product of the current and voltage represents the power output for that operating condition. A solar cell can also be characterised by its *maximum power point*, when the product $V_{mp} \times I_{mp}$ is at its maximum value. The maximum power output of a cell is graphically given by the largest rectangle that can be fitted under the I-V curve. That is,

$$\frac{d(IV)}{dV} = 0$$

giving

$$V_{mp} = V_{oc} - \frac{nkT}{q}\ln\left(\frac{V_{mp}}{(nkT/q)}+1\right) \qquad (3.4)$$

For example, if $n = 1.3$ and $V_{oc} = 600$ mV, as for a typical silicon cell, V_{mp} is about 93 mV smaller than V_{oc}.

The power output at the maximum power point under strong sunlight (1 kW/m^2) is known as the 'peak power' of the cell. Hence photovoltaic panels are usually rated in terms of their 'peak' watts (W$_p$).

The *fill factor* (*FF*), is a measure of the junction quality and series resistance of a cell. It is defined as

$$FF = \frac{V_{mp}I_{mp}}{V_{oc}I_{sc}} \qquad (3.5)$$

Hence

$$P_{mp} = V_{oc}I_{sc}FF \qquad (3.6)$$

Obviously, the nearer the fill factor is to unity, the higher the quality of the cell. Ideally, it is a function only of the open circuit voltage and can be calculated using the approximate empirical expression (Green, 1982)

$$FF = \frac{v_{oc} - \ln(v_{oc}+0.72)}{v_{oc}+1} \qquad (3.7)$$

where v_{oc} is defined as a 'normalised V_{oc}'; that is

$$v_{oc} = \frac{V_{oc}}{(nkt/q)} \qquad (3.8)$$

The above expression applies to *ideal cases* only, with no parasitic resistance losses, and is accurate to about one digit in the fourth decimal place for these cases.

3.2 SPECTRAL RESPONSE

Solar cells respond to individual photons of incident light by absorbing them to produce an electron-hole pair, provided the photon energy (E_{ph}) is greater than the bandgap energy (E_g). Photon energy in excess of E_g is quickly dissipated as heat, as shown in Fig. 3.6.
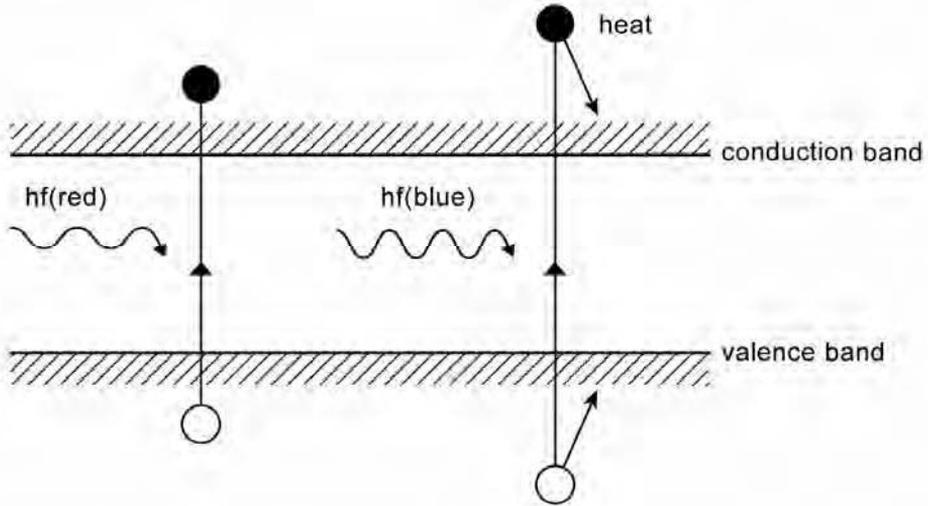
Figure 3.6. The creation of electron-hole pairs and dissipation of energy in excess of E_g.

The quantum efficiency (QE) of a solar cell is defined as the number of electrons moving from the valence band to the conduction band per incident photon. The longest wavelength for which this is finite is limited by its bandgap. Maximum use can only be made of incoming sunlight if the bandgap is in the range 1.0–1.6 eV. This effect alone acts to limit the maximum achievable efficiency of solar cells to 44% (Shockley & Queisser, 1961). The bandgap of silicon, at 1.1 eV, is close to optimum, while that of gallium arsenide, at 1.4 eV, is even better, in principle. Fig. 3.7 illustrates the dependence of ideal quantum efficiency on bandgap.

Also of interest is the spectral responsivity of a solar cell, given by the amperes generated per watt of incident light (Fig. 3.8). Ideally, this increases with wavelength. However, at short wavelengths, cells cannot use all the energy in the photons, whereas at long wavelengths, the weak absorption of light means that most photons are absorbed a long way from the collecting junction and the finite diffusion length in the cell material limits the cell's response.

Spectral responsivity (SR) can be calculated as follows:

$$SR = \frac{I_{sc}}{P_{in}(\lambda)} = \frac{q \times n_e}{\frac{hc}{\lambda} \times n_{ph}} = \frac{q\lambda}{hc} EQE \qquad (3.9)$$

where n_e is the flux of electrons, per unit time, flowing in an external circuit at short circuit conditions and I_{sc} is the short circuit current, n_{ph} is the flux of photons of wavelength λ incident on the cell per unit time, P_{in} is the incident light power and $EQE = (1 - R) \times IQE$ is the external efficiency, which differs from the internal quantum efficiency (IQE) in that the latter excludes the fraction, R, of light reflected from the top surface. $SR \rightarrow 0$ as $\lambda \rightarrow 0$, since there are fewer photons in each watt of incident light.

This strong wavelength dependence of responsivity makes cell performance in turn strongly dependent on the spectral content of sunlight. In addition, optical and recombination losses mean that actual cells can only approach these ideals.
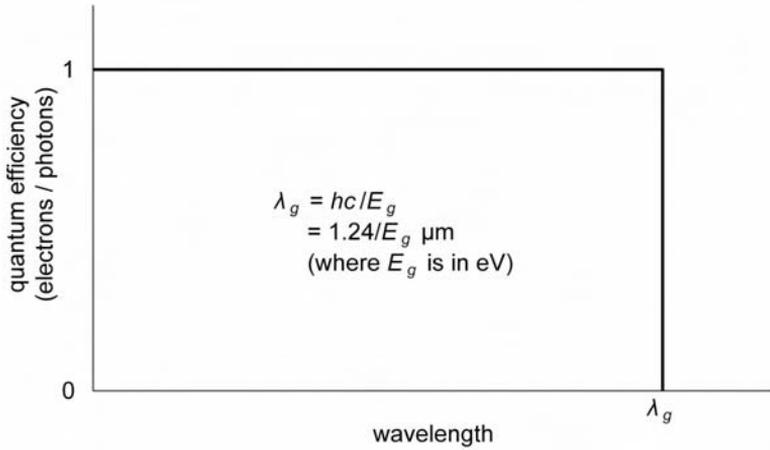
Figure 3.7. Bandgap limitations on the quantum efficiency of silicon solar cells.
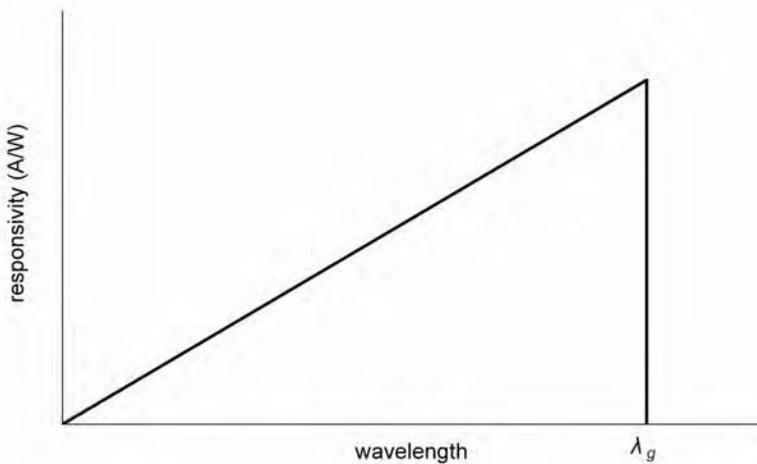
Figure 3.8. The quantum limit of spectral responsivity as a function of wavelength.

3.3   EFFECT OF TEMPERATURE

The operating temperature of a solar cell is determined by the ambient air temperature, by the characteristics of the module in which it is encapsulated (see Section 5.8), by the intensity of sunlight falling on the module, and by other variables such as wind velocity.

The dark saturation current I_0 increases with temperature according to the equation

$$I_0 = BT^\gamma \exp\left(\frac{-E_{g0}}{kT}\right) \tag{3.10}$$

where B is independent of temperature, E_{g0} is the linearly extrapolated zero temperature bandgap of the semiconductor making up the cell (Green, 1992) and γ includes the temperature dependencies of the remaining parameters determining I_0.

The short circuit current (I_{sc}) increases with temperature, since the bandgap energy (E_g) decreases and more photons have enough energy to create e-h pairs. However, this is a small effect. For silicon

$$\frac{1}{I_{sc}}\frac{dI_{sc}}{dT} \approx +0.0006 \,°\mathrm{C}^{-1} \tag{3.11}$$

The main effect of increasing temperature for silicon solar cells is a reduction in V_{oc}, the fill factor and hence the cell output. These effects are illustrated in Fig. 3.9.
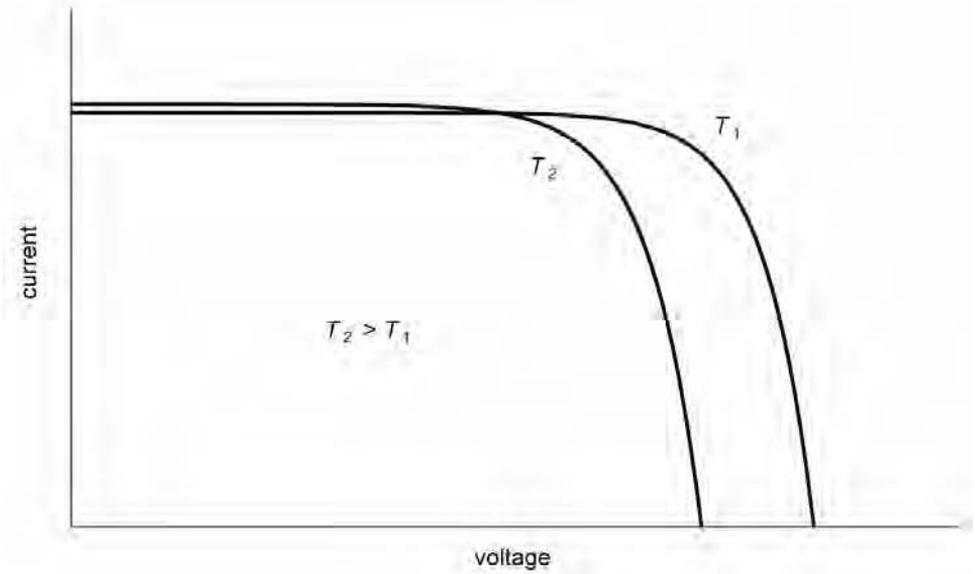
Figure 3.9. The effect of temperature on the I-V characteristics of a solar cell.

The temperature dependency of V_{oc} and FF for silicon is approximated by the following equations:

$$\frac{dV_{oc}}{dT} = \frac{-\left[V_{g0} - V_{oc} + \gamma(kT/q)\right]}{T} \approx -2 \text{ mV/°C} \tag{3.12}$$

$$\frac{1}{V_{oc}}\frac{dV_{oc}}{dT} \approx -0.003 \,°\mathrm{C}^{-1} \tag{3.13}$$

50

$$\frac{1}{FF}\frac{d(FF)}{dT} \approx \frac{1}{6}\left[\frac{1}{V_{oc}}\frac{dV_{oc}}{dT} - \frac{1}{T}\right] \approx -0.0015\,°\text{C}^{-1} \qquad (3.14)$$

For silicon, the effect of temperature on the maximum power output (P_{mp}) is as follows:

$$\frac{1}{P_{mp}}\frac{dP_{mp}}{dT} \approx -(0.004 \sim 0.005)\,°\text{C}^{-1} \qquad (3.15)$$

The higher the value of V_{oc}, the smaller the expected temperature dependence. Temperature effects are discussed in detail by Emery *et al.* (1996), King *et al.* (1997) and Radziemska (2003).

3.4 EFFECT OF PARASITIC RESISTANCES

Solar cells generally have a parasitic series and shunt resistance associated with them, as shown in Fig. 3.10. Both types of parasitic resistance act to reduce the fill-factor.
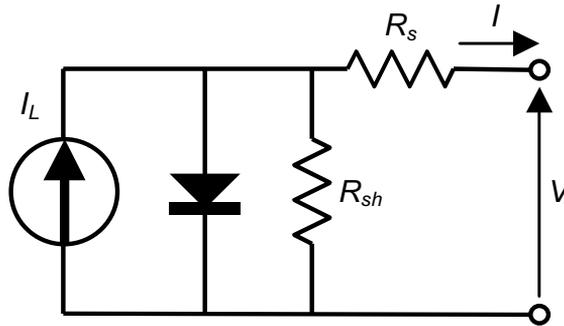
Figure 3.10. Parasitic series and shunt resistances in a solar cell circuit.

The major contributors to the series resistance (R_s) are the bulk resistance of the semiconductor material, the metallic contacts and interconnections, carrier transport through the top diffused layer, and contact resistance between the metallic contacts and the semiconductor. The effect of series resistance is shown in Fig. 3.11.
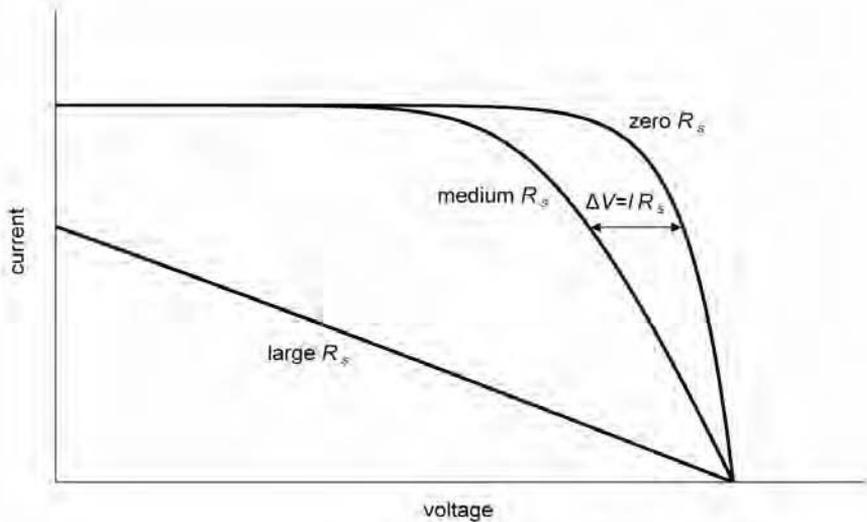
Figure 3.11. The effect of series resistance on fill factor.

The shunt resistance (R_{sh}) is due to *p-n* junction non-idealities and impurities near the junction, which cause partial shorting of the junction, particularly near cell edges. The effect of shunt resistance is shown in Fig. 3.12.
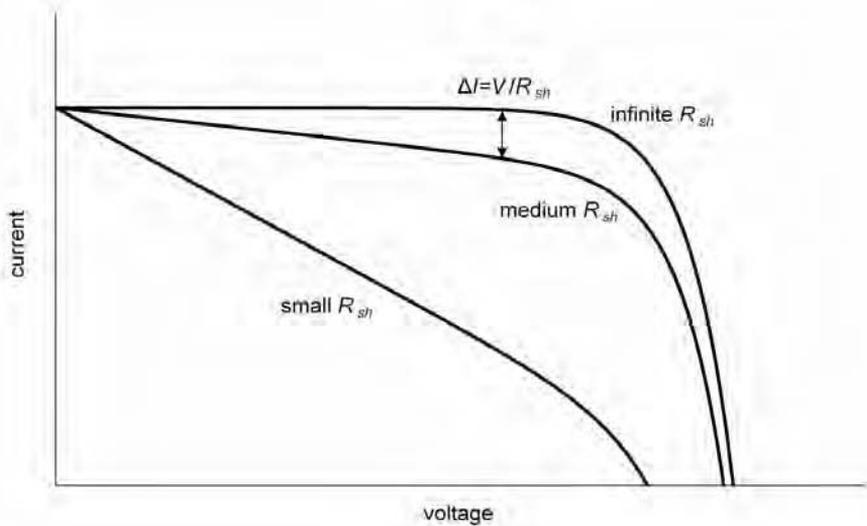
Figure 3.12. The effect of shunt resistance on fill factor in a solar cell.

Since the fill factor determines the power output of the cell, the maximum power output is related to the series resistance, as given approximately by

$$P_m \approx \left(V'_{mp} - I'_{mp} R_s \right) I'_{mp}$$

$$\approx P_{mp} \left(1 - \frac{I'_{mp}}{V'_{mp}} R_s \right)$$

$$\approx P_{mp} \left(1 - \frac{I_{sc}}{V_{oc}} R_s \right).$$

If the characteristic resistance of a solar cell is defined as (Green, 1982)

$$R_{ch} = \frac{V_{oc}}{I_{sc}} \tag{3.17}$$

it is possible to define a 'normalised R_s' such that

$$r_s = \frac{R_s}{R_{ch}} \tag{3.18}$$

Hence

$$FF \approx FF_0 \left(1 - r_s \right) \tag{3.19}$$

or, empirically but more accurately

$$FF_s \approx FF_0 \left(1 - 1.1 r_s \right) + \frac{r_s^{\,2}}{5.4} \tag{3.20}$$

which is valid for $r_s < 0.4$ and $v_{oc} > 10$.

Similarly, for shunt resistance, it is possible to define

$$r_{sh} = \frac{R_{sh}}{R_{ch}} \tag{3.21}$$

Then, as before

$$FF \approx FF_0 \left(1 - \frac{1}{r_{sh}} \right) \tag{3.22}$$

or, again more accurately (Green, 1992)

$$FF_{sh} = FF_0 \left[1 - \frac{v_{oc} + 0.7}{v_{oc}} \frac{FF_0}{r_{sh}} \right] \tag{3.23}$$

which is valid for $r_{sh} > 0.4$.

In the presence of both series and shunt resistances, the I-V curve of a solar cell is given by

$$I = I_L - I_0 \left[\exp\left(\frac{V + IR_s}{(nkT/q)} \right) - 1 \right] - \frac{V + IR_s}{R_{sh}} \qquad (3.24)$$

To combine the effect of both series and shunt resistances, the expression for FF_{sh}, derived above, can be used, with FF_0 replaced by FF_s (Green, 1992).

EXERCISES

3.1   (a)   Taking the silicon bandgap as 1.12 eV, and assuming unity quantum efficiency as in Figs. 3.7 and 3.8, calculate the upper limit on the short circuit current density of a silicon solar cell at 300 K for the standard 'unnormalised' global AM1.5 spectrum supplied in tabulated form in Appendix B.

      (b)   Given that, near operating temperatures, the silicon bandgap decreases by 0.273 mV/°C, calculate the normalised temperature coefficient of this current limit at 300 K

$$\frac{1}{I_{sc}} \frac{dI_{sc}}{dT}$$

3.2   (a)   A silicon solar cell (bandgap 1.12 eV) is uniformly illuminated by monochromatic light of wavelength 800 nm and intensity 20 mW/cm^2. Given that its quantum efficiency at this wavelength is 0.80, calculate the short circuit current of the cell if its area is 4 cm^2.

      (b)   For the same quantum efficiency, what would be the value of this current if the cell were made from a semiconductor of bandgap (i) 0.7 eV, (ii) 2.0 eV.

      (c)   For the silicon cell of part (a), calculate the open circuit voltage, fill factor and energy conversion efficiency, given that its ideality factor is 1.2 and dark saturation current density is 1 pA/cm^2.

      (d)   Estimate the range of values of (i) series resistance and (ii) shunt resistance that would cause a relative reduction in the fill factor and energy conversion efficiency of less than 5%.

3.3   (a)   When the cell temperature is 300 K, a certain silicon cell of 100 cm^2 area has an open circuit voltage of 600 mV and a short circuit current of 3.3 A under 1 kW/m^2 illumination. Assuming that the cell behaves ideally, what is its energy conversion efficiency at the maximum power point?

      (b)   What would be its corresponding efficiency if the cell had a series resistance of 0.1 Ω and a shunt resistance of 3 Ω?

REFERENCES

Emery, K., Burdick, J., Caiyem, Y., Dunlavy, D., Field, H., Kroposki, B. & Moriarty, T. (1996), in Proc. 25th IEEE Photovoltaic Specialists Conference, Washington, 13–17 May 1996, IEEE, New York, pp. 1275–1278.

Green, M.A. (1982), 'Accuracy of analytical expressions for solar cell fill factors', *Solar Cells*, **7**, pp. 337–340.

Green, M.A. (1992), *Solar Cells: Operating Principles, Technology and System Applications*, University of NSW, Kensington, Australia.

King, D. L., Kratochvil, J. A. & Boyson, W. E. (1997), in Proc. 26th IEEE Photovoltaic Specialists Conference, Anaheim, 30 September–3 October 1997, IEEE, New York, pp. 1183–1186.

Radziemska, E. (2003), 'The effect of temperature on the power drop in crystalline silicon solar cells', *Renewable Energy*, **28**(1), pp. 1–12.

Shockley, W. & Queisser, H.J. (1961), 'Detailed balance limit of efficiency of *p-n* junction solar cells', *Journal of Applied Physics*, **32**, pp. 510–519.